Available online at www.sciencedirect.com
ScienceDirect
Chemical Physics 327 (2006) 512–517
Chemical Physics
www.elsevier.com/locate/chemphys

Accommodation of ethanol, acetone and benzaldehyde by the liquid–vapor interface of water: A molecular dynamics study

Sébastien Canneaux [a], Jean-Christophe Soetens [b], Eric Henon [a], Frédéric Bohr [a,*]

[a] Equipe de Chimie Théorique Appliquée, UMR CNRS 6089, Université de Reims Champagne-Ardenne, UFR Sciences Exactes et Naturelles, Moulin de la Housse, BP 1039, 51687 Reims Cedex 2, France
[b] Laboratoire de Physico-Chimie Moléculaire, UMR CNRS 5803, Université de Bordeaux I, 351, Cours de la Libération, 33405 Talence Cedex, France

Received 7 February 2006; accepted 25 May 2006
Available online 29 June 2006

Abstract

In the atmosphere, the interaction of volatile organic compounds (VOCs) with liquid droplets is still poorly understood, but it must be included in atmospheric models for a better description of the atmospheric (tropospheric and stratospheric) chemistry. In this study, we have used molecular dynamics simulations to examine the insertion of three VOCs (ethanol, acetone and benzaldehyde) into the liquid–vapor interface of water (using the SPC/E water model). Our results are in agreement with the theoretical studies available in the literature. At 298 and 273 K, we have calculated theoretical mass accommodation coefficients from the Gibbs free energy profiles corresponding to the insertion of each VOC into the water interface. These calculations lead to a theoretical mass accommodation coefficient equal to 1.0 for each examined VOC at both temperatures.
© 2006 Elsevier B.V. All rights reserved.

Keywords: Molecular dynamics simulation; Ethanol; Acetone; Benzaldehyde; Gibbs free energy profile; Mass accommodation coefficient; Heterogeneous atmospheric chemistry; Volatile organic compounds

1. Introduction

The troposphere contains a great part of the atmospheric water, as well as a large part of the gas phase of the atmosphere. Moreover, volatile organic compounds (VOCs) which are emitted from the surface of the earth, such as ethanol, acetone, or benzaldehyde, are retained in this area of the atmosphere. Ethanol is widely used as a solvent and as fuel additive. Its emissions accounted for about 4%, by mass, of anthropogenic emissions of VOCs in UK in 1993 [1]. Concerning acetone, it is a dominant VOC compound present in rural forested regions with mixing ratios that often exceed those observed in urban areas [2]. Benzaldehyde can be found in fruits and is used, for example, in the manufacturing of deodorants/air fresheners. Benzaldehyde belongs to the family of aromatic aldehydes which are major contributors to the air pollution [1].

In the atmosphere, VOCs can react with free radicals. For example, the acetone molecule can react with the OH radical [3–8]. On the other hand, the presence of water drops (atmospheric clouds) in the troposphere can involve multiphasic chemistry [9]. The existence of acid rains confirms the important role of the aerosols in atmospheric chemistry [10]. Reactions in condensed phase or heterogeneous reactions can provide alternative reactional mechanisms compared to those occurring in homogeneous gas phase [11]. Moreover, studies of such reactions are of great interest in atmospheric sciences to predict the lifetime of soluble species [12].

The non-reactive uptake process of a molecule by a water drop consists of: (1) the diffusion of the molecule in gas phase towards the liquid–vapor interface, (2) the

* Corresponding author.
E-mail addresses: jc.soetens@lpcm.u-bordeaux1.fr (J.-C. Soetens), frederic.bohr@univ-reims.fr (F. Bohr).

0301-0104/$ - see front matter © 2006 Elsevier B.V. All rights reserved.
doi:10.1016/j.chemphys.2006.05.033

transport across the liquid–vapor interface, and (3) the diffusion in the liquid (bulk of water) from the interface. The adsorption of molecules at the liquid–vapor interface is an important step in the uptake process of atmospheric pollutants by a water drop [13–20]. Indeed, once the molecule is adsorbed at the liquid–vapor interface, it can be desorbed or remains adsorbed on the interface or enters into the bulk of water.

The probability so that a molecule striking the surface is accommodated by a liquid water drop is represented by the mass accommodation coefficient α

$$\alpha = \frac{\text{number of molecules entering the liquid phase}}{\text{number of molecular collisions with the surface}} \leqslant 1$$

This accommodation is treated commonly as a two-step process: (1) the gas molecules strike the surface then they are adsorbed, and (2) the species can enter into the bulk of water. Consequently, if α is equal to the unity, each molecule striking the surface enters into the liquid and is not desorbed.

The mass accommodation coefficient for a species M is interpreted using a simple kinetic model [21]

$$[\mathrm{M}]_{\mathrm{g}} \underset{k_{\mathrm{desorb}}}{\overset{k_{\mathrm{adsorb}}}{\rightleftarrows}} [\mathrm{M}]_{\mathrm{ad}} \overset{k_{\mathrm{solv}}}{\rightarrow} [\mathrm{M}]_{\mathrm{solv}}$$

Here, $[\mathrm{M}]_{\mathrm{g}}$, $[\mathrm{M}]_{\mathrm{ad}}$, and $[\mathrm{M}]_{\mathrm{solv}}$ represent the gas, adsorbed and solvated concentrations of the species M, respectively. k_{adsorb}, k_{desorb} and k_{solv} represent the rate constants for adsorption at the interface, desorption (into the gas phase) and solvation, respectively. Note that the kinetic model assumes: (1) the absence of liquid saturation and (2) that a gas phase molecule strikes the surface with unit probability. Thus, the mass accommodation, α, can be defined from the probability that the molecule will be solvated versus desorbed back into the gas phase [21]. It can be determined by using the following formula

$$\frac{\alpha}{1-\alpha} = \frac{k_{\mathrm{solv}}}{k_{\mathrm{desorb}}} = \frac{\exp\left(\frac{-\Delta G^{\ddagger}_{\mathrm{solv}}}{RT}\right)}{\exp\left(\frac{-\Delta G^{\ddagger}_{\mathrm{desorb}}}{RT}\right)} = \exp\left(-\frac{\Delta(\Delta G^{\ddagger})}{RT}\right) \qquad (1)$$

Here, R is the ideal gas constant. $\Delta G^{\ddagger}_{\mathrm{solv}}$ and $\Delta G^{\ddagger}_{\mathrm{desorb}}$ are the activation Gibbs free energy for solvation and desorption, respectively (as shown in Fig. 1). The activation Gibbs free energy ($\Delta(\Delta G^{\ddagger})$) can be regarded as the Gibbs free energy of the transition state between gas phase and solvation. Using the aforementioned chemical kinetic model, experimental results [13–16,18,20] show that the insertion process has a large Gibbs free energy barrier between the adsorbed state of the molecule (at the interface) and the state where the molecule is inside the water drop.

When the VOC is far from the water surface, there is no interaction between the VOC and the liquid–vapor interface. Therefore, when the VOC approaches the interface, the Gibbs free energy does not vary. The interactions between the water interface and the VOC molecule are very weak and are negligible (on a distance range between the VOC and the interface): only the water molecules interact together. Once the VOC is close to the water surface, additional interactions are observed between the VOC and the molecules of water in the gas phase and then, the VOC forms hydrogen bonds with some water molecules. The Gibbs free energy decreases until the organic molecule is adsorbed at the interface. The molecule must then create a cavity to enter into the liquid, resulting in an increase in the Gibbs free energy. Once the molecule is entered, it diffuses in the liquid. Layers of solvation are created all around it, what results in a reduction of the Gibbs free energy.

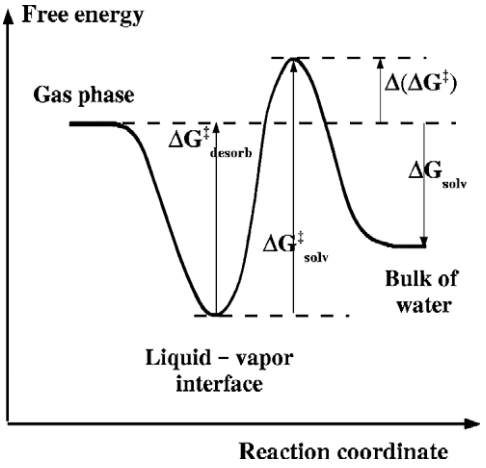

Fig. 1. Schematic Gibbs free energy profile for the insertion of a molecule from the gas phase into the bulk of water.

Taylor et al. [22] made molecular dynamics simulations to explore the structural and dynamical properties of the liquid–vapor interface of SPC/E [23] water lamella. The calculated surface tension of H_2O [22] compares favorably with the corresponding experimental measurements. Furthermore, Taylor et al. made molecular dynamics simulations to examine the accommodation of an ethanol, an ethylene glycol and a water molecule by a bulk of water (using the SPC/E model) [24,25]. Ethanol and ethylene glycol are bound to the surface of H_2O with adsorption Gibbs free energies of -30.1 and -38.1 kJ mol^{-1} (at 298 K), respectively, and the calculated mass accommodation coefficient has been determined, using the above kinetic model, to be unity. Wilson et al. [26] calculated the Gibbs free energy profiles for the solvation of methanol and ethanol across the water liquid–vapor interface of TIP4P [27] water lamella. In their study, they determined a mass accommodation coefficient equal to the unity. Very recently, the review article by Garrett et al. [28] show that molecular dynamics on compounds that are very water soluble is going to predict a mass accommodation coefficient of unity.

However, these theoretical results are not in agreement with the corresponding small experimental mass accommodation coefficients. The use of the above kinetic description

of the accommodation process to interpret these experimental values, shows that a Gibbs free energy barrier should exist between the state of the solute in the bulk of water and the state of the solute adsorbed at the interface [13,21], being larger than the Gibbs free energy of desorption.

The aim of this work was to determine the theoretical mass accommodation coefficients for ethanol, acetone and benzaldehyde in liquid water. We have compared them with those previously calculated for ethanol, ethylene glycol and methanol. With respect to previous works (simulations of alcohol insertions) [24–26,29], two other organic functions have been examined.

2. Computational details

In our simulations, the SPC/E water model developed by Berendsen et al. [23] was used. Indeed, this model correctly represents the surface tension and the structural properties of the water liquid–vapor interface [22,30]. Concerning the three studied volatile organic compounds (ethanol, acetone and benzaldehyde), we have used the OPLS Lennard–Jones parameters [31–33]. The atom-centered charges were calculated (except for ethanol, for which we have used the charges of Jorgensen et al. [32]) with the Gaussian 98 program [34]. These charges were calculated using a Merz–Kollman electrostatic potential fit [35,36] at the RHF/6-31G(d)//MP2/6-31G(d,p) level of theory. The COV-H_2O intermolecular parameters were determined by using the OPLS mixing rules [37].

Calculations were carried out using the microcanonic (NVT) ensemble (where the number of molecules, volume and temperature are constant). Two temperatures were considered in the present study, 273 and 298 K and all simulations were performed using the MDpol program [38]. A simulation cell containing 456 water molecules is increased in one direction (according to the z direction) on both sides of 25 Å to create the vacuum (see Fig. 2). The simulation box lengths in the x, y and z directions are 23.9, 23.9 and 71.4 Å, respectively. The center of mass (COM) of water molecules is maintained in the geometrical center of the cell throughout the simulation. Periodic boundary conditions were applied in the three directions and a cutoff distance of 11.9 Å were used. A step size of 0.002 ps was employed. This simulation cell was then equilibrated during 1 ns in order to form the liquid–vapor interface.

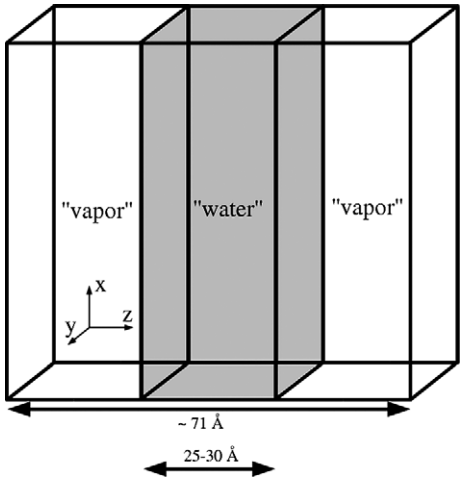

Fig. 2. Simulation cell.

The VOC was positioned initially at 20 Å of the COM of water molecules, in the vacuum part of the simulation cell. This new simulation cell was reequilibrated during 500 ps by holding the position of the COM solute in its initial position (the x, y, z COM of solute were constant). In other words, only the rotational movements of the COV molecule were allowed.

In this work, we have determined the Gibbs free energy curves corresponding to the COV insertion into the bulk of water at both temperatures. These curves can be obtained by using the thermodynamic perturbation approach [39,40]. Statistical mechanical perturbation theory has been widely used to calculate the potential of mean force (PMF) for the association of two entities in a bath of solvent molecules (see Refs. [41–43], for example). The PMFs were computed with the Gibbs free energy perturbation (FEP) method [40], in which the Gibbs free energy difference between two states, "0" and "1", is obtained from the following equation:

$$\Delta G = G_1 - G_0 = -RT \ln\langle \exp -(U_1 - U_0)/RT \rangle_0 \quad (2)$$

where T is the temperature of the system, U_1 and U_0 are the potential energies of the states "1" and "0", respectively.

Because the Gibbs free energy difference to bring the solute from 20 Å (initial state) to the COM of the water molecules (final state) is large, the total reaction pathway is divided into N contiguous substates connected by means of a coupling parameter, λ_i, which is related to the distance between the COM solute and the COM water molecules, $r(\lambda)$ via

$$\Delta G = \sum_{i=1}^{N-1} \Delta G_i \quad (3)$$

where ΔG_i is defined from (2) by

$$\Delta G_i = -RT \ln\langle \exp -(U_{\lambda_{i-1}} - U_{\lambda_i})/RT \rangle_{\lambda_i} \quad (4)$$

In this work, a reaction coordinate was defined (the distance between the COM solute and the COM water molecules) perpendicularly to the liquid–vapor interface. This reaction coordinate was divided into 50 windows of 0.4 Å. For each step, along the reaction coordinate, a molecular dynamics simulation was carried out (each simulation was equilibrated for 50 ps prior to a 200 ps trajectory in which energetic data were collected).

First, we present in the following section, the results concerning the properties of the liquid–vapor interface of water. Next, we show (at 298 K) the Gibbs free energy profile corresponding to the accommodation of one ethanol molecule into a water lamella and we compare it with the

theoretical profiles given in the literature [24,25]. These calculations have validated our methodology. We have used this methodology at 273 and 298 K to calculate the Gibbs free energy profiles corresponding to the accommodation of one acetone molecule and one benzaldehyde molecule into a water lamella.

Concerning the simulations at 273 K, we present the average Gibbs free energy profiles of four PMF simulations, to have a better sampling.

3. Results and discussion

First, we have carried out two molecular dynamics simulations, at 298 K, to explore the properties of the liquid–vapor interface (see Fig. 3), using the effective SPC/E water model [23] and polarizable PSPC water model [44]. Fig. 3 shows the water molecules density profile and the average total dipole moment of water molecules (as a function of z coordinate). Concerning the SPC/E water molecules density profile, the density (d) is equal to 1 g cm^{-3} in the liquid phase, and equal to 0 g cm^{-3} in the vacuum. Our liquid phase density is in very good agreement with the results of Berendsen et al. ($d = 0.99$ g cm^{-3}) [23]. Between these two domains (liquid phase and gas phase), the distance range where the density decreases from 1 to 0 g cm^{-3} indicates that the thickness of the liquid–vapor interface is about 5 Å. The maximum of the density profile obtained using the PSPC water model is also in agreement with the original results of Ahlström et al. ($d = 0.99$ g cm^{-3}) [44]. The use of this polarizable model allows to examine the change of the total dipole moment of the water molecules from the bulk to the gas phase. Our results show that the molecules located in the middle of the lamella ($z = 0$) are polarized like in the liquid ($\mu = 3.0$ D as in Ref. [44]). Moreover, going from the bulk to the gas phase, the average total dipole moment decreases continuously down to the dipole moment of an isolated water molecule ($\mu = 1.8$ D). These results indicate that the thickness of the water lamella used in the present study is sufficient to modelise the phenomena of interest, *i.e.*. the insertion of a molecule into liquid water. The use of an effective water model such as SPC/E introduces approximations in predicting properties of the interface but allows to perform long simulations due to its simplicity. The effect of polarizability on the Gibbs free energy profile in our systems could be the subject of a future study.

Jayne et al. [13] carried out experimental studies relating to the uptake of solutes into a water drop, and in particular, the uptake of ethanol. The results were interpreted in term of a Gibbs free energy barrier between the solute in the gas phase and solvation. For ethanol, the mass accommodation coefficient ($\alpha = 0.048$ at 273 K) was obtained from these experimental results. In order to obtain the theoretical mass accommodation coefficient for ethanol, we have carried out the insertion of an ethanol molecule on both sides of the water lamella (dashed lines in Fig. 4). Fig. 4 shows the water molecules density profile (solid line), two Gibbs free energy profiles (dashed lines) and the average Gibbs free energy profile (bold dashed line) at 298 and 273 K. Note that "$w(z)$" (the reversible work), in Fig. 4, corresponds to the difference in the Gibbs free energy between two successive values of the reaction coordinate. The zero in energy is defined when the solute is far from the liquid–vapor interface. For each temperature, the two Gibbs free energy profiles are in good agreement.

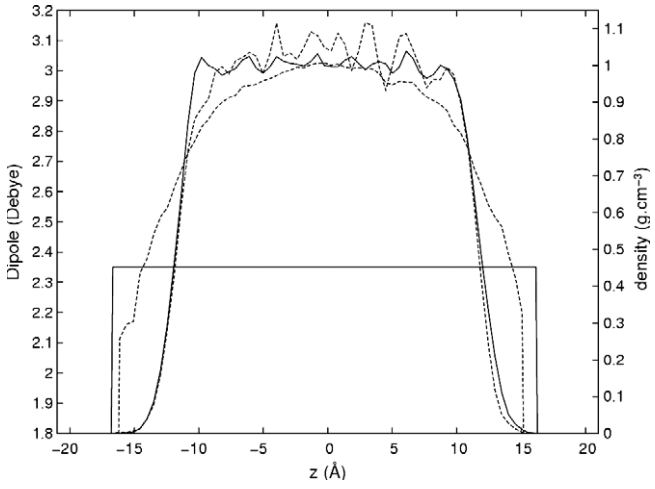

Fig. 3. Average total dipole moment of water molecules and density profile of water at 298 K as a function of z coordinate for two water models. Solid line: results from a MD simulation using the effective SPC/E water model [23]; dashed line: results from a MD simulation using the polarizable PSPC water model [44].

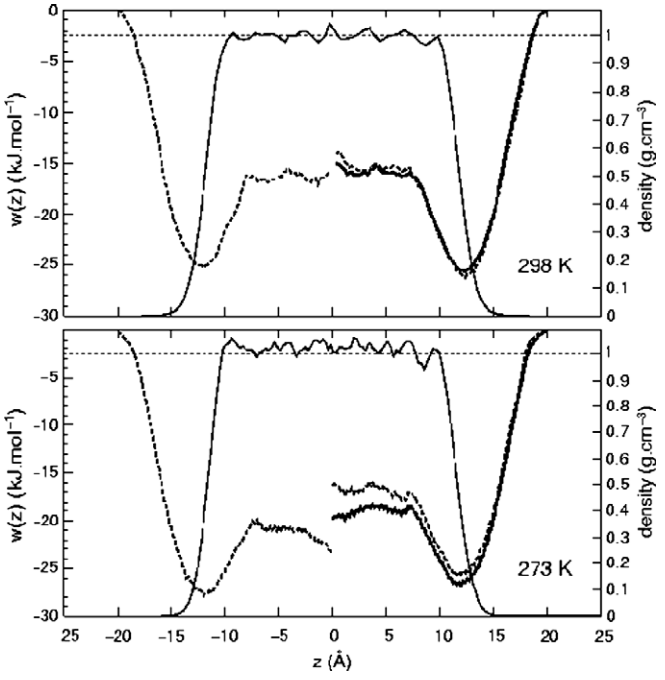

Fig. 4. Potential of mean force corresponding to the insertion of an ethanol molecule into water at 298 and 273 K and associated density profile of water. Solid line: water density profile; dashed line: potential of mean force for *up* or *down* approach and in bold dashed line the average potential of mean force.

As we can see in Table 1, at 298 K, our calculated solvation Gibbs free energy of ethanol, $\Delta G_{solv} = -15.9$ kJ mol^{-1} (which corresponds to the end point of the liquid curves), is in agreement with the experimental results of Wagman et al. ($\Delta G_{solv} = -21.1$ kJ mol^{-1} at 298 K) [45] and the theoretical results of Taylor et al. ($\Delta G_{solv} = -24.3$ kJ mol^{-1} at 298 K) [24,25] and those of Wilson and Pohorille ($\Delta G_{solv} = -21.8$ kJ mol^{-1} at 310 K) [26]. The difference observed between our computed value and the previous theoretical results, certainly results from the use of different force fields. Consequently, we feel confident that our potential correctly describes the H_2O–ethanol energetics.

The values of $\Delta G^{\ddagger}_{desorb}$ and $\Delta(\Delta G^{\ddagger})$ (Table 1) are predicted to be 25.5 and -15.9 kJ mol^{-1}, respectively. These results are in accordance with the theoretical results of Taylor et al. ($\Delta G^{\ddagger}_{desorb} = 30.1$ kJ mol^{-1} and $\Delta(\Delta G^{\ddagger}) = -22.6$ kJ mol^{-1}) [24,25]. Using our $\Delta(\Delta G^{\ddagger})$ value, the mass accommodation coefficient is calculated to be 1.0. These first results, concerning the ethanol insertion into a water lamella, are consistent with the theoretical results of the literature and validate our methodology. However, it is important to note that no Gibbs free energy barrier was found above the reactant Gibbs free energy level between the adsorbed state of the molecule and the state where the molecule is inside the bulk of water. This result agrees favorably with the molecular dynamics simulations of Taylor et al. [24] which show a similar behavior. The corresponding experimental value for the mass accommodation coefficient can be estimated to be 0.0093 at 298 K from data in Ref. [13], and results in an experimental value of $\Delta(\Delta G^{\ddagger})$ of 11.7 kJ mol^{-1} (using Eq. (1)). This is 27.6 kJ mol^{-1} larger than our calculated value.

The Gibbs free energy curves for the insertion of ethanol into the water lamella at 273 K are shown in Fig. 4. At 273 K, the values of $\Delta G^{\ddagger}_{desorb}$, $\Delta(\Delta G^{\ddagger})$, ΔG_{solv} and α were determined to be 26.8, -18.8, -20.1 kJ mol^{-1} and 1.0, respectively (see Table 1). The issued theoretical mass accommodation coefficient (1.0), disagrees with the small experimental Jayne et al.'s value (0.048 at 273 K) [13], but is in accordance with the theoretical values (1.0) of Taylor et al. [24,25] and Wilson et al. [26]. Moreover, Jayne et al. [13] showed that there was a negative temperature dependence of the mass accommodation coefficient, *i.e.* at low temperatures, more molecules are accommodated than at higher temperatures. This is in line with our theoretical result, *i.e.* decreasing the temperature lowers the Gibbs free energy barrier ($\Delta(\Delta G^{\ddagger}) = -15.9$ kJ mol^{-1} at 298 K and $\Delta(\Delta G^{\ddagger}) = -18.8$ kJ mol^{-1} at 273 K).

Table 1
Energetic data (kJ mol^{-1}) and mass accommodation coefficients for the insertion of ethanol, acetone and benzaldehyde into a bulk of water, at 298 and 273 K

	$\Delta G^{\ddagger}_{desorb}$	$\Delta(\Delta G^{\ddagger})$	ΔG_{solv}	α
$T = 298$ K				
Ethanol	25.5	−15.9	−15.9	1.0
Acetone	25.5	−16.3	−16.7	1.0
Benzaldehyde	28.9	−15.9	−17.2	1.0
$T = 273$ K				
Ethanol	26.8	−18.8	−20.1	1.0
Acetone	26.8	−17.6	−17.6	1.0
Benzaldehyde	29.3	−18.8	−20.5	1.0

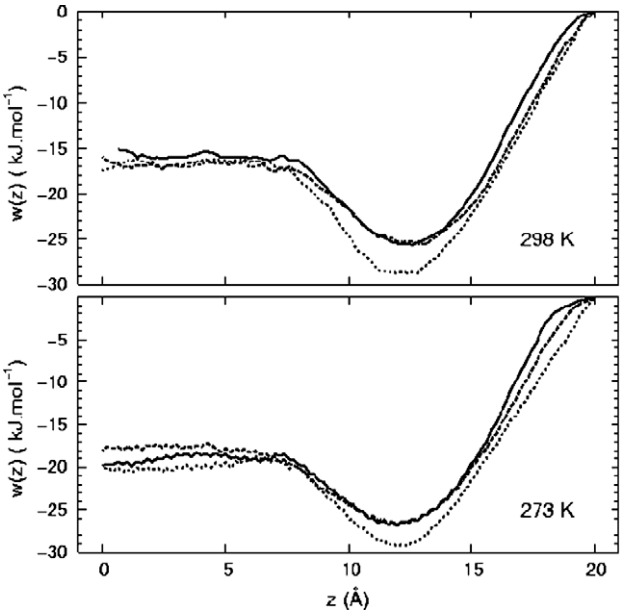

Fig. 5. Potential of mean force corresponding to the insertion of an ethanol molecule (solid line), acetone molecule (dashed line) and benzaldehyde molecule (dotted line) into water at 298 and 273 K.

We have also examined the insertion of the acetone and the benzaldehyde molecules at 298 and 273 K (see Fig. 5). We report in Table 1, the corresponding values for $\Delta G^{\ddagger}_{desorb}$, $\Delta(\Delta G^{\ddagger})$, ΔG_{solv} and α. As we can see, these values are of the same order of magnitude as those obtained for the ethanol insertion. Our calculated solvation Gibbs free energies for acetone, at 273 K ($\Delta G_{solv} = -17.6$ kJ mol^{-1}) and 298 K ($\Delta G_{solv} = -16.7$ kJ mol^{-1}) are in agreement with the experimental results of Nathanson et al. ($\Delta G_{solv} = -21.1$ kJ mol^{-1} at 273 K and $\Delta G_{solv} = -19.2$ kJ mol^{-1} at 298 K) [17]. Nathanson et al. [17] and Leyssens [20] determined an experimental mass accommodation coefficient (α) of 0.026 at 273 K for acetone, and 0.0002 at 293 K for benzaldehyde, respectively. Substituting our $\Delta(\Delta G^{\ddagger})$ for acetone and benzaldehyde in Eq. (1) at both temperatures, the resulting mass accommodation coefficients are predicted to be 1.0. These results disagree with the aforementioned experimental values as for in the ethanol case.

4. Conclusion

We have calculated the Gibbs free energy profiles for the insertion of ethanol, acetone and benzaldehyde molecules into a liquid–vapor interface of water at 298 and 273 K. Our profiles at 298 K for ethanol agree with the theoretical results of Taylor et al. [24,25], validating our methodology. To our knowledge, there are no theoretical data for acetone and benzaldehyde. The mass accommodation coefficients

estimated to be 1.0 at both temperatures (298 and 273 K) are not in accordance with the experimental results ($\alpha \ll 1$). The reason is that no Gibbs free energy barrier was predicted between the adsorbed state of the molecule (at the interface) and the state where the molecule is inside the water drop.

Consequently, the difference between the experimental and the theoretical results must be understood by carrying out other calculations. Taylor et al. [25] have made improvements in estimating the non-equilibrium effects on the barrier of solvation for ethanol in water using the Grote–Hynes theory. In other respects, Stewart et al. [29] studied the insertion of an ethanol molecule into a saturated (by ethanol molecules) liquid–vapor interface. But the question for this discrepancy with experiments remains [28].

In further studies, the description of the liquid–vapor interface could be improved by using a polarizable water model in order to account for the variation of the dipole moment of the water molecules (in the bulk and into the liquid–vapor interface). Also, simulations of the insertion of clusters (of the type COV-$(H_2O)_n$) into the interface would be useful to describe the accommodation process. Indeed, in their experimental and theoretical studies, Katrib et al. [12] showed that clusters are formed at the interface before they enter into the bulk of water.

Acknowledgements

I.D.R.I.S., C.I.N.E.S, C.R.I.H.A.N. and the computational centre (ROMEO) of the Universite of Reims-Champagne-Ardenne are acknowledged for the CPU time donated. We are particularly grateful to the Region Champagne-Ardenne for financial support.

References

[1] R.G. Derwent, M.E. Jenkin, S.M. Saunders, Atmos. Environ. 30 (1996) 181.
[2] A.H. Goldstein, G.W. Schade, Atmos. Environ. 34 (2000) 4997.
[3] G. Vasvari, I. Szilagyi, A. Bencsura, S. Dobé, T. Bérces, E. Henon, S. Canneaux, F. Bohr, Phys. Chem. Chem. Phys. 3 (2001) 551.
[4] E. Henon, S. Canneaux, F. Bohr, S. Dobé, Phys. Chem. Chem. Phys. 5 (2003) 333.
[5] S. Canneaux, E. Henon, F. Bohr, React. Kinet. Catal. Lett. 82 (1) (2004) 105.
[6] S. Canneaux, N. Sokolowski-Gomez, E. Henon, F. Bohr, S. Dobé, Phys. Chem. Chem. Phys. 6 (2004) 5172.
[7] T. Gierczak, M.K. Gilles, S. Bauerle, A.R. Ravishankara, J. Phys. Chem. A 107 (2003) 5014.
[8] R.K. Talukdar, T. Gierczak, D.C. McCabe, A.R. Ravishankara, J. Phys. Chem. A 107 (2003) 5021.
[9] T.E. Graedel, K.I. Goldberg, J. Geophys. Res. 88 (1983) 10865.
[10] J.H. Seinfeld, S.N. Pandis, Atmospheric Chemistry and Physics: From Air Pollution to Climate Change, John Wiley & Sons, 1998.
[11] J.P. Reid, R.M. Sayer, Chem. Soc. Rev. 32 (2003) 70.
[12] Y. Katrib, Ph. Mirabel, S. Le Calvé, G. Weck, E. Kochanski, J. Phys. Chem. B 106 (2002) 7237.
[13] J.T. Jayne, S.X. Duan, P. Davidovits, D.R. Worsnop, M.S. Zahniser, C.E. Kolb, J. Phys. Chem. 95 (1991) 6329.
[14] D.R. Worsnop, M.S. Zahniser, C.E. Kolb, J.A. Gardner, L.R. Watson, J.M. Van Doren, J.T. Jayne, P. Davidovits, J. Phys. Chem. 93 (1989) 1159.
[15] J.M. Van Doren, L.R. Watson, P. Davidovits, D.R. Worsnop, M.S. Zahniser, C.E. Kolb, J. Phys. Chem. 94 (1990) 3265.
[16] J.T. Jayne, S.X. Duan, P. Davidovits, D.R. Worsnop, M.S. Zahniser, C.E. Kolb, J. Phys. Chem. 96 (1992) 5452.
[17] G.M. Nathanson, P. Davidovits, D.R. Worsnop, C.E. Kolb, J. Phys. Chem. 100 (1996) 13007.
[18] M. Schütze, H. Herrmann, Phys. Chem. Chem. Phys. 6 (2004) 965.
[19] G. Leyssens, F. Louis, J.-P. Sawerysyn, J. Phys. Chem. A 109 (2005) 1864.
[20] G. Leyssens, Ph.D. Thesis, University of Lille I, 2004.
[21] P. Davidovits, J.T. Jayne, S.X. Duan, D.R. Worsnop, M.S. Zahniser, C.E. Kolb, J. Phys. Chem. 95 (1991) 6337.
[22] R.S. Taylor, L.X. Dang, B.C. Garrett, J. Phys. Chem. 100 (1996) 11720.
[23] H.J.C. Berendsen, J.R. Grigera, T.P. Straatsma, J. Phys. Chem. 91 (1987) 6269.
[24] R.S. Taylor, D. Ray, B.C. Garrett, J. Phys. Chem. B 101 (1997) 5473.
[25] R.S. Taylor, B.C. Garrett, J. Phys. Chem. B 103 (1999) 844.
[26] M.A. Wilson, A. Pohorille, J. Phys. Chem. B 101 (1997) 3130.
[27] W.L. Jorgensen, J. Chandrasekhar, J.D. Madura, R.W. Impey, M.L. Klein, J. Chem. Phys. 79 (1983) 926.
[28] B.C. Garrett, G.K. Schenter, A. Morita, Chem. Rev. 106 (2006) 1355.
[29] E. Stewart, R.L. Shields, S. Taylor, J. Phys. Chem. B 107 (2003) 2333.
[30] J. Alejandre, D.J. Tildesley, G.A. Chapela, J. Chem. Phys. 102 (1995) 4574.
[31] W.L. Jorgensen, J.D. Madura, C.J. Swenson, J. Am. Chem. Soc. 106 (1984) 6638.
[32] W.L. Jorgensen, J. Phys. Chem. 90 (1986) 1276.
[33] H.A. Carlson, T.B. Nguyen, M. Orozco, W.L. Jorgensen, J. Comput. Chem. 14 (1993) 1240.
[34] M.J. Frisch, G.W. Trucks, H.B. Schlegel, G.E. Scuseria, M.A. Robb, J.R. Cheeseman, V.G. Zakrzewski, J.A. Montgomery Jr., R.E. Stratmann, J.C. Burant, S. Dapprich, J.M. Millam, A.D. Daniels, K.N. Kudin, M.C. Strain, O. Farkas, J. Tomasi, V. Barone, M. Cossi, R. Cammi, B. Mennucci, C. Pomelli, C. Adamo, S. Clifford, J. Ochterski, G.A. Petersson, P.Y. Ayala, Q. Cui, K. Morokuma, P. Salvador, J.J. Dannenberg, D.K. Malick, A.D. Rabuck, K. Raghavachari, J.B. Foresman, J. Cioslowski, J.V. Ortiz, A.G. Baboul, B.B. Stefanov, G. Liu, A. Liashenko, P. Piskorz, L. Komaromi, R. Gomperts, R.L. Martin, D.J. Fox, T. Keith, M.A. Al-Laham, C.Y. Peng, A. Nanayakkara, M. Challacombe, P.M.W. Gill, B. Johnson, W. Chen, M.W. Wong, J.L. Andres, C. Gonzalez, M. Head-Gordon, E.S. Replogle, J.A. Pople, Gaussian 98, Revision A.11, Gaussian Inc., Pittsburgh, PA, 2001.
[35] B.H. Besler, K.M. Merz, P.A. Kollman, J. Comput. Chem. 11 (1990) 431.
[36] U.C. Singh, P.A. Kollman, J. Comput. Chem. 5 (1984) 129.
[37] A.R. Leach, Molecular Modelling: Principles and Applications, second ed., Pearson Education Limited, 2001.
[38] J.-C. Soetens, Ph.D. Thesis, University of Nancy I, 1996.
[39] J.G. Kirkwood, J. Chem. Phys. 3 (1935) 300.
[40] R.W. Zwanzig, J. Chem. Phys. 22 (1954) 1420.
[41] S.E. Huston, P.J. Rossky, D.A. Zichi, J. Am. Chem. Soc. 111 (1989) 5680.
[42] D.E. Smith, L.X. Dang, J. Chem. Phys. 100 (1994) 3757.
[43] J.-C. Soetens, C. Millot, C. Chipot, G. Jansen, J.G. Angyan, B. Maigret, J. Phys. Chem. B 101 (1997) 10910.
[44] P. Ahlström, A. Wallqvist, S. Engström, B. Jönsson, Mol. Phys. 68 (1989) 563.
[45] D.D. Wagman, W.H. Evans, V.B. Parker, S.M. Baley, R.H. Shumm, Natl. Bur. Stand. (US) Technical Note 270-3, 1968.